



## Charge-storage performance of Li/LiFePO<sub>4</sub> cells with additive-incorporated ionic liquid electrolytes at various temperatures



Nithinai Wongittharom<sup>a</sup>, Chueh-Han Wang<sup>b</sup>, Yi-Chen Wang<sup>a,b</sup>, George Ting-Kuo Fey<sup>a</sup>, Hui-Ying Li<sup>b</sup>, Tzi-Yi Wu<sup>c</sup>, Tai-Chou Lee<sup>a,1</sup>, Jeng-Kuei Chang<sup>a,b,\*</sup>

<sup>a</sup>Department of Chemical and Materials Engineering, National Central University, Taiwan

<sup>b</sup>Institute of Materials Science and Engineering, National Central University, Taiwan

<sup>c</sup>Department of Chemical and Materials Engineering, National Yunlin University of Science and Technology, Taiwan

### HIGHLIGHTS

- Ionic liquid (IL) electrolytes show high thermal stability and non-flammability.
- Effects of electrolyte additives are systematically studied at various temperatures.
- At 25 °C, γ-butyrolactone is an effective additive to improve cell performance.
- Above 50 °C, the electrolyte additives are not necessary.
- No capacity loss was found after 100 cycles at 75 °C in the plain IL electrolyte.

### ARTICLE INFO

#### Article history:

Received 8 November 2013

Received in revised form

10 February 2014

Accepted 24 February 2014

Available online 6 March 2014

#### Keywords:

Lithium battery

Electrolyte

Ionic liquid

Additive

Temperature

### ABSTRACT

Butylmethylpyrrolidinium bis(trifluoromethanesulfonyl)imide (BMP-TFSI) ionic liquid (IL) with LiTFSI solute is used as a base electrolyte for Li/LiFePO<sub>4</sub> cells. Three kinds of electrolyte additive, namely vinylene carbonate (VC), gamma-butyrolactone (γ-BL), and propylene carbonate (PC), with various concentrations are introduced. The thermal stability, flammability, and electrochemical properties of the electrolytes are investigated. At 25 °C, the additives (γ-BL is found to be the most effective) can significantly improve the capacity, high-rate performance, and cyclability of the cells. With an increase in temperature to 50 °C, the benefits of the additives gradually become insignificant. At 75 °C, the additives even have adverse effects. At such an elevated temperature, in the plain IL electrolyte (without additives), a LiFePO<sub>4</sub> capacity of 152 mAh g<sup>-1</sup> is found at 0.1 C. 77% of this capacity can be retained when the rate is increased to 3 C. These values are superior to those found for the additive-incorporated IL and conventional organic electrolytes. Moreover, negligible capacity loss is measured after 100 charge–discharge cycles at 75 °C in the plain IL electrolyte.

© 2014 Elsevier B.V. All rights reserved.

### 1. Introduction

Lithium (Li) batteries are the dominant charge-storage units for consumer portable electronic devices due to their high energy density and satisfactory cycle life [1]. They are also quite promising for next-generation hybrid and electric vehicles [2–5], and are

being considered for grid-scale energy storage for renewable wind and solar power [6]. One major concern for Li batteries extended to further applications (especially for large-scale batteries) is safety [7]. Commonly used organic electrolytes are responsible for the safety threat since they have poor thermal stability and high flammability. These electrolytes also pose environmental hazards due to their volatility and toxicity [8,9]. Accordingly, a safer and greener alternative electrolyte, namely ionic liquid (IL), which is characterized by intrinsic conductivity, large electrochemical windows, excellent stability, non-volatility, and non-flammability [8,10–15], has attracted a lot of attention.

Although IL electrolytes have many advantages, their relatively high viscosity compared to that of conventional organic electrolytes

\* Corresponding author. 300 Jhong-da Road, National Central University, Taoyuan, Taiwan. Tel.: +886 3 4227151x34908; fax: +886 3 2805034.

E-mail addresses: [taichoulee@ncu.edu.tw](mailto:taichoulee@ncu.edu.tw) (T.-C. Lee), [jkchang@ncu.edu.tw](mailto:jkchang@ncu.edu.tw) (J.-K. Chang).

<sup>1</sup> Tel.: +886 3 4227151x34211.

makes them unfavorable for use in high-C-rate applications. Several additives, such as zwitterionic compounds [16–18], poly(ethylene glycol) dimethyl ether [19,20], propylene carbonate (PC) [21,22], vinylene carbonate (VC) [23,24], and gamma-butyrolactone ( $\gamma$ -BL) [25,26], have thus been introduced into IL electrolytes. The functions of the additives include a reduction of the IL electrolyte viscosity [27] (thus increasing the ionic conductivity [28]) and facilitation of the formation of a stable electrode/electrolyte interface film to prevent undesirable electrode damage [29]. Thorough performance comparisons between various additives in IL electrolytes, however, have not been conducted. Moreover, a fixed additive concentration is usually adopted in the literature, which provides relatively limited information. These issues are considered in this study.

Since the IL viscosity can be significantly reduced and the  $\text{Li}^+$  mobility can be remarkably enhanced [30,31] with increasing temperature, IL electrolytes should be promising (versus organic electrolytes, which have low thermal stability) for elevated-temperature Li battery applications. However, systematic studies on the effects of temperature on cell performance (such as capacity, rate capability, and cycle life) with IL electrolytes and comparisons with conventional organic electrolyte cells, though of great importance, have not been made. In addition, how IL additives work at various temperatures is still unknown. These issues are rather critical and need to be clarified before IL-electrolyte Li batteries can be practically deployed.

In this study, butylmethylpyrrolidinium–bis(trifluoromethyl sulfonyl)imide (BMP–TFSI) IL is used as a base electrolyte because its cathodic stability limit (associated with the reduction of  $\text{BMP}^+$ ) is beyond the Li plating/stripping reaction and  $\text{TFSI}^-$  can withstand a high potential (>5.5 V vs. Li) [32]. This IL is thus a promising electrolyte candidate for Li-metal batteries. LiTFSI, which has been confirmed to be more suitable than  $\text{LiPF}_6$  [33], is dissolved in the IL to allow  $\text{Li}^+$  transport. Three types of additive, namely VC,  $\gamma$ -BL, and PC, with various concentrations were introduced into the IL electrolyte for Li/LiFePO<sub>4</sub> cells. The cell performance was evaluated at 25 °C, 50 °C, and 75 °C. The experimental results indicate that at 75 °C, the IL electrolyte clearly outperforms the conventional organic electrolyte. The additives, which are desirable at 25 °C, have adverse effects at elevated temperatures.

## 2. Experimental procedure

### 2.1. Preparation of LiFePO<sub>4</sub> powder and ionic liquid electrolytes

Carbon-coated LiFePO<sub>4</sub> powder was prepared using a carbo-thermal reduction method at 700 °C involving a mixture of ferric oxide (99%, Taiwan Polychem Co. Ltd.), ammonium dihydrogen phosphate (99%, First Chemical Works Co. Ltd.), and lithium carbonate (99%, First Chemical Works Co. Ltd.) in the required stoichiometric ratio. In the preparation process, polyethylene glycol (PEG, M.W. = 6000, Huacheng Industrial Co. Ltd.) was used as a reduction agent as well as a carbon source. The detailed synthesis procedures can be found in a previous paper [34]. BMP–TFSI IL was prepared and purified following a published method [35]. The IL was washed with dichloromethane (99%, SHOWA), filtered to remove precipitates, and then vacuum-dried at 100 °C for 12 h before use. The water content, measured using a Karl Fisher titrator, was below 100 ppm. 1 M LiTFSI (98%, Tokyo Chemical Industry Co. Ltd.) was dissolved into the IL to allow  $\text{Li}^+$  transport. VC (C<sub>2</sub>H<sub>3</sub>O<sub>2</sub>, 97%, Alfa Aesar),  $\gamma$ -BL (C<sub>4</sub>H<sub>6</sub>O<sub>2</sub>, 97%, ECHO), and PC (C<sub>4</sub>H<sub>6</sub>O<sub>3</sub>, 99.7%, Sigma-Aldrich) were used as the electrolyte additives. Each mixture was continuously stirred by a magnetic paddle for 24 h to ensure uniformity. A conventional organic electrolyte, consisting of 1:1 (by volume) ethylene carbonate (99%, Alfa Aesar) and diethyl

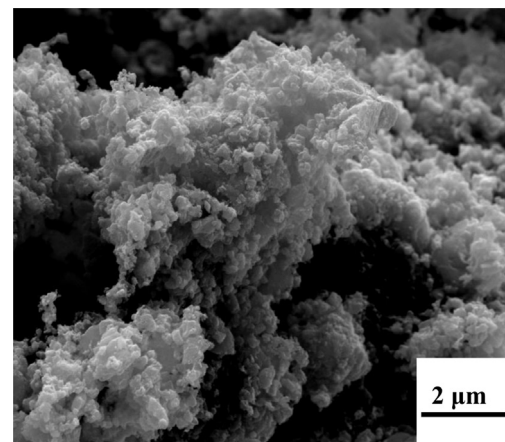


**Fig. 1.** SEM micrograph of LiFePO<sub>4</sub> powder synthesized using a PEG-assisted carbo-thermal reduction method.

carbonate (99%, Alfa Aesar) as co-solvent and 1 M  $\text{LiPF}_6$  solute, was also prepared for comparison. All the chemicals were stored and handled in an argon-filled glove box (Innovation Technology Co. Ltd.), where both the moisture content and oxygen content were maintained below 1 ppm.

The electrolyte conductivity was measured using a conductivity meter (TetraCon 325) in the glove box to avoid oxygen and moisture interference. The  $\text{Li}^+$  transference number,  $T_{\text{Li}}^+$ , in the IL electrolyte was determined by a dc polarization method combined with impedance spectroscopy, as proposed by Bruce and Evans et al. [36,37]. Briefly, a small polarization ( $\Delta V$ , 40 mV) was applied to a symmetrical Li/electrolyte/Li cell and then the initial current ( $I_0$ ) and steady-state current ( $I_{ss}$ ) were Li electrodes were also examined. The  $T_{\text{Li}}^+$  can be calculated according to:

$$T_{\text{Li}}^+ = \frac{I_{ss} \Delta V - I_0 R_0}{I_0 \Delta V - I_s R_s}$$

### 2.2. Cell assembly

A cathode slurry was prepared by mixing 75 wt% synthesized LiFePO<sub>4</sub> powder, 20 wt% carbon black, and 5 wt% poly(vinylidene fluoride) in N-methyl-2-pyrrolidone solution. The slurry was pasted onto Al foil and vacuum-dried at 110 °C for 2 h. Then, the cathode electrode was roll-pressed and punched to match the

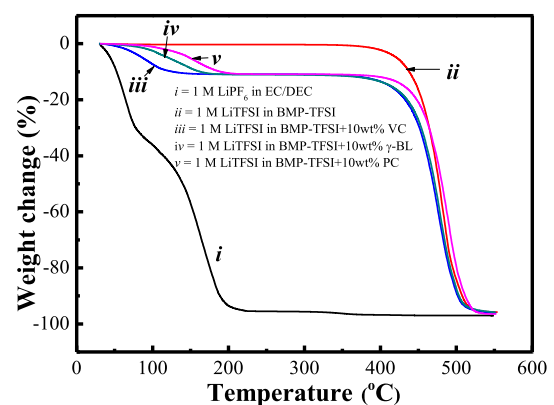


**Fig. 2.** TGA data of a conventional organic electrolyte (1 M  $\text{LiPF}_6$  in EC:DEC (1:1, v/v) solvent) and IL electrolytes without and with 10 wt% VC,  $\gamma$ -BL, and PC, respectively. The measurements were performed at a heating rate of 5 °C min<sup>-1</sup> under a nitrogen atmosphere.

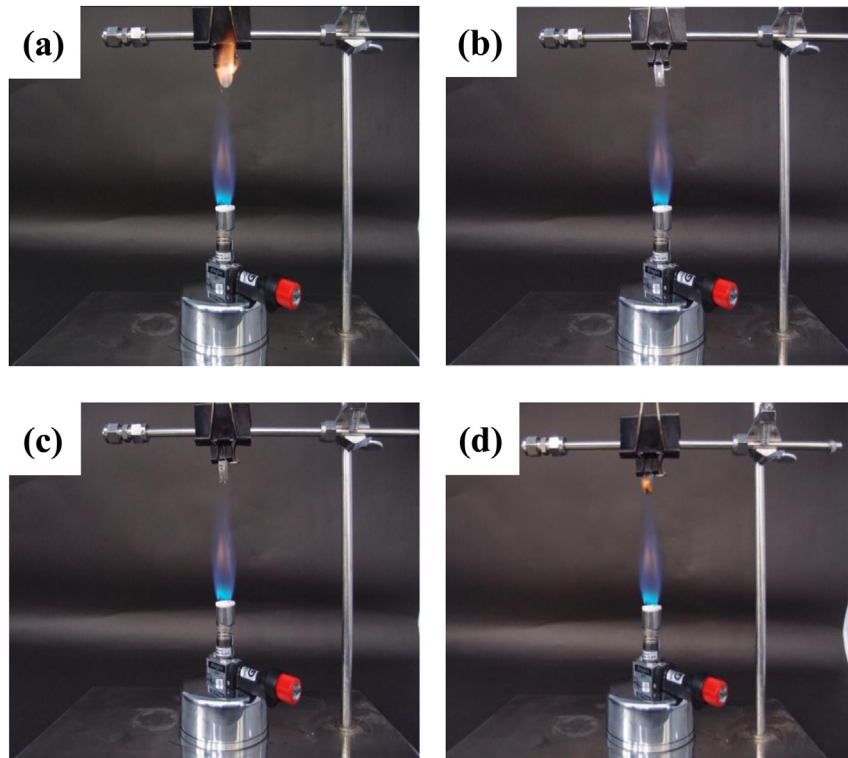


**Fig. 3.** Flammability tests of (a) 1 M  $\text{LiPF}_6$  in EC:DEC (1:1, v/v) organic electrolyte, (b) plain IL electrolyte, (c) IL electrolyte with 10 wt% VC, and (d) IL electrolyte with 15 wt% VC.

required dimensions of a CR2032 coin cell. Li foil and a Celgard polypropylene membrane were used as the anode and the separator, respectively. The assembly of coin cells was conducted in the argon-filled glove box.

### 2.3. Material and electrochemical characterizations

The morphology of the synthesized  $\text{LiFePO}_4$  was examined with a scanning electron microscope (SEM; FEI Inspect F50). An X-ray diffractometer (XRD; Bruker D8 Advance) with a Cu target was used to analyze the crystal structure. The X-ray detector was scanned in a diffraction angle range of  $15^\circ$ – $65^\circ$  at a speed of  $1^\circ \text{ min}^{-1}$ . A thermogravimetric analyzer (TGA; Perkin–Elmer TGA7) was employed to examine the thermal stability of the electrolytes. The samples were heated from room temperature to  $550^\circ\text{C}$  at a heating rate of  $5^\circ\text{C min}^{-1}$  under a nitrogen atmosphere. The electrolyte flammability was tested under air according to an established method in

the literature [10]. Briefly, glassy fiber filters were used to adsorb the electrolytes and then burned with an electric Bunsen burner (with a distance of 120 mm between the sample and the burner). The charge–discharge performances (such as capacity, high-rate capability, and cyclic stability) of the  $\text{Li}/\text{LiFePO}_4$  cells with various electrolytes were evaluated at  $25^\circ\text{C}$ ,  $50^\circ\text{C}$ , and  $75^\circ\text{C}$  (in a cell voltage range of 2.0–4.5 V) using a battery tester (Arbin BT-2043).

## 3. Results and discussion

The surface morphology of the prepared  $\text{LiFePO}_4$  powder is shown in Fig. 1. As shown in the SEM micrograph, the agglomerated phosphate clusters ( $\sim 5 \mu\text{m}$  in diameter) consist of numerous sub-grains. The primary particle size was in a range of 100–200 nm, which is smaller than that of the  $\text{LiFePO}_4$  powder synthesized using different processes [38–41]. This can be attributed to the presence of PEG during the preparation process refining the

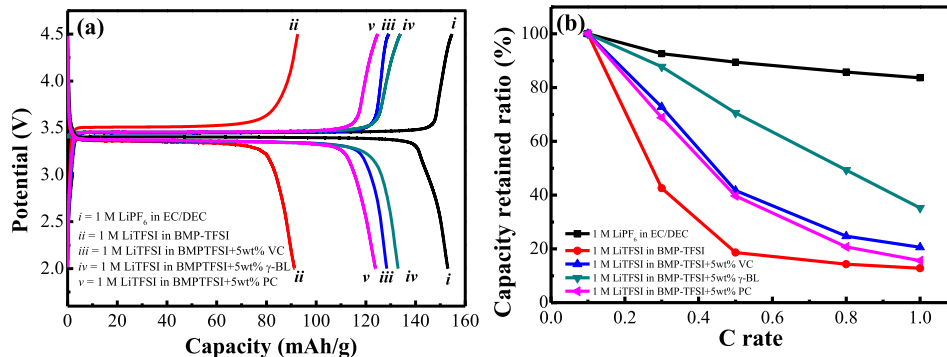


**Fig. 4.** (a) Charge–discharge curves at 0.1 C and (b) capacity retained ratios at various charge–discharge rates compared to that obtained at 0.1 C of  $\text{Li}/\text{LiFePO}_4$  cells incorporating a conventional organic electrolyte and IL electrolytes without and with 5 wt% VC,  $\gamma$ -BL, and PC, respectively, at  $25^\circ\text{C}$ .

morphology and causing the size reduction of the powder [34]. It has been confirmed that a small size of LiFePO<sub>4</sub> can shorten the Li<sup>+</sup> diffusion pathway and thus improve the charge–discharge performance of the electrode [42]. The XRD analysis (see Supplementary Data, Fig. S1) indicates that the obtained powder shows a single olivine phase with an orthorhombic structure (JCPDS 40-1499). This result confirms that the Fe<sub>2</sub>O<sub>3</sub> precursor was completely reduced (by PEG) and that no impurity phase formed during the synthesis. The surface carbon film (for promoting electronic conduction) on the LiFePO<sub>4</sub> powder was recognized from an X-ray photoelectron spectroscopy analysis (see Supplementary Data, Fig. S2).

Fig. 2 shows the TGA data of various electrolytes. The plain IL electrolyte (without additives) shows negligible weight change before the decomposition temperature of ~400 °C, indicating excellent thermal stability. For the IL electrolytes with 10 wt% VC, γ-BL, and PC, clear weight loss associated with evaporation of the organic additives began at around 65 °C, 95 °C, and 115 °C, respectively. When the boiling points of VC (132 °C), γ-BL (204 °C), and PC (242 °C) were reached, all the additives (10 wt%) were completely removed and the electrolyte weight became stable before the IL decomposition. In contrast, the traditional organic electrolyte showed a significant weight loss of ~40% before 100 °C, at which point the carbonate solvent vigorously evaporated and the LiPF<sub>6</sub> started to decompose into LiF and PF<sub>5</sub> [43,44]. These results clearly reveal that IL electrolytes are more suitable for high-temperature applications.

The flammability tests of various electrolytes (typically 0.1 g) were performed under air. The results are shown in Fig. 3. While the organic electrolyte (Fig. 3(a)) ignited immediately and burned rather violently, the ILs without and with 10 wt% VC (Fig. 3(b) and (c), respectively) did not show any ignition even when directly exposed to fire. After the burner was removed, the average self-extinguishing time of the organic electrolyte (10 samples) was ~60 s g<sup>-1</sup>. When 15 wt% VC was introduced (Fig. 3(d)), there was a 50% possibility (according to 10 tests) of ignition, although the flame was less violent and the self-extinguishing time was shorter (~5 s g<sup>-1</sup>) than those of the conventional organic electrolyte. Similar phenomena were found for the γ-BL- and PC-incorporated IL electrolytes, suggesting that the additives should not be added in excessive amounts when battery safety is a concern.

Fig. 4(a) compares the charge–discharge voltage profiles of the Li/LiFePO<sub>4</sub> cells (at 0.1 C) with various electrolytes at 25 °C. In the conventional organic electrolyte, the measured capacity of LiFePO<sub>4</sub> was 153 mAh g<sup>-1</sup>, which is close to the theoretical value

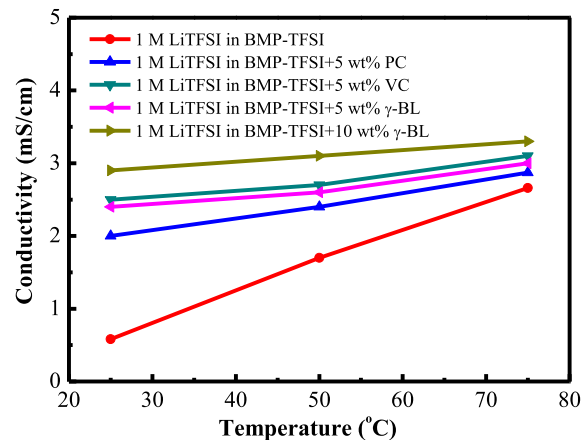


Fig. 6. Conductivity values of the IL electrolytes without and with various additives measured at 25, 50, and 50 °C.

of 170 mAh g<sup>-1</sup> [45]. This indicates that the synthesized electrode is of high quality. The capacity found in the plain IL is only 91 mAh g<sup>-1</sup>, due to the high viscosity (thus inferior conductivity) of the electrolyte. However, as shown, the LiFePO<sub>4</sub> capacities remarkably increased to 128, 133, and 123 mAh g<sup>-1</sup>, respectively, when 5 wt% VC, γ-BL, and PC were added. The capacity retained ratios of the cells at various charge–discharge C rates (based on that obtained at 0.1 C) are shown in Fig. 4(b). Clearly, the high-rate performance is significantly enhanced by the electrolyte additives. At 1 C, 13%, 21%, 35%, and 16% of the capacity was retained for the IL cells without and with 5 wt% VC, γ-BL, and PC additives, respectively. γ-BL is less viscous than PC, and thus there is a higher diffusion coefficient of Li<sup>+</sup> in the former solution [46]. Our study indicates that γ-BL is the best of the three additives. Figs. 5 and 6 show the viscosity and conductivity, respectively, of the ILs without and with various additives. Moreover, the measured  $T_{Li}^+$  values are given in Table 1. While the VC-incorporated IL exhibits the lowest viscosity and the highest conductivity, the γ-BL-incorporated IL has the largest  $T_{Li}^+$  among the electrolytes. Electrochemical impedance spectroscopic analyses of the Li/LiFePO<sub>4</sub> cells were also conducted (see Supplementary Data, Fig. S3); the results indicated that the additive clearly reduced the electrolyte resistance (but slightly increased the charge-transfer resistance). As shown in Fig. 4, although incorporation of the additives effectively improves the cell performance at 25 °C, the high-rate capability of the cells with the IL-based electrolytes is still inferior to that of a similar cell with a conventional organic electrolyte.

The effects of the γ-BL concentration in the IL electrolyte on the cell performance were further studied. As shown in Fig. 7(a), the measured discharge capacities at 0.1 C and 25 °C are 124, 133, 140,

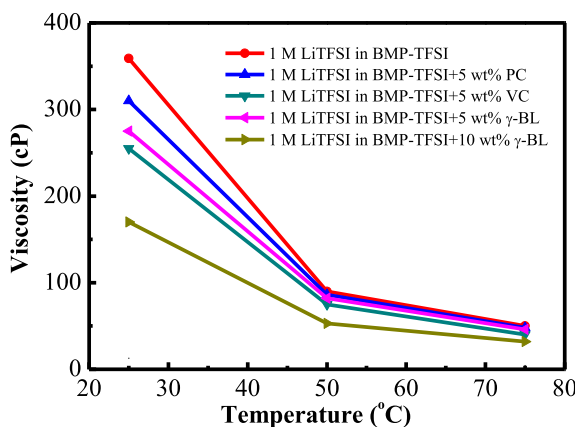
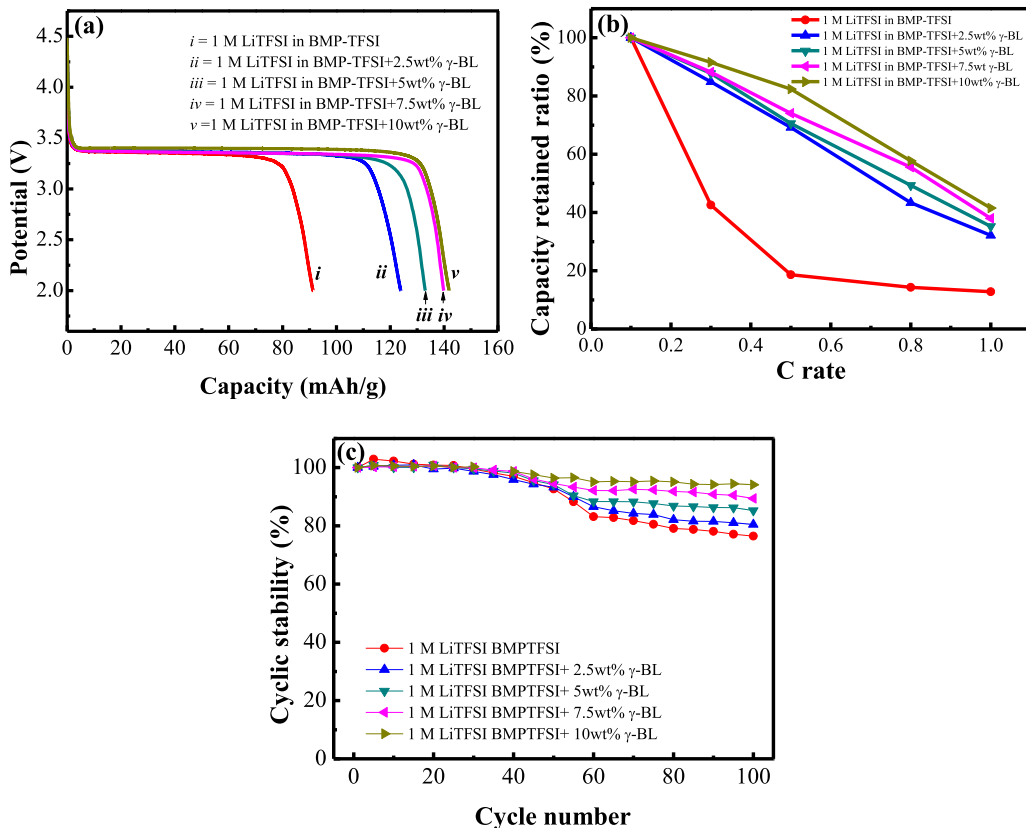


Fig. 5. Viscosity values of the IL electrolytes without and with various additives measured at 25, 50, and 50 °C.

**Table 1**  
 $Li^+$  transference numbers,  $T_{Li}^+$ , in various electrolytes at 25 and 50 °C.

Temperature	Electrolyte	$T_{Li}^+$
25 °C	Neat IL electrolyte	0.28
	IL electrolyte with 5 wt% PC	0.34
	IL electrolyte with 5 wt% VC	0.35
	IL electrolyte with 5 wt% γ-BL	0.37
	IL electrolyte with 10 wt% γ-BL	0.38
	Neat IL electrolyte	0.35
50 °C	IL electrolyte with 5 wt% PC	0.39
	IL electrolyte with 5 wt% VC	0.39
	IL electrolyte with 5 wt% γ-BL	0.41
	IL electrolyte with 10 wt% γ-BL	0.42



**Fig. 7.** (a) Discharge curves at 0.1 C, (b) capacity retained ratios at various charge-discharge rates compared to that obtained at 0.1 C, and (c) cyclic stability of Li/LiFePO<sub>4</sub> cells incorporating IL electrolytes without and with various concentrations of  $\gamma$ -BL at 25 °C.

and 142 mAh g<sup>-1</sup>, respectively, for  $\gamma$ -BL concentrations of 2.5, 5, 7.5, and 10 wt%. The capacity retained ratios at high rates are shown in Fig. 7(b). Clearly, increasing the  $\gamma$ -BL amount led to an enhanced rate capability, because of the increase in conductivity (as Fig. 6) and  $T_{\text{Li}}^+$  (as Table 1) of the electrolyte. The same phenomenon was found for the VC additive (see Supplementary Data, Fig. S4). Table 2 compares the performance of the  $\gamma$ -BL and VC additives at various concentrations, confirming that the former is more effective in the IL electrolyte to increase the cell capacity and high-rate performance.

Fig. 7(c) shows the cyclic stability of the cells with various electrolytes at 25 °C. With increasing  $\gamma$ -BL concentration in the IL electrolyte, the charge–discharge stability gradually improved. After 100 cycles, the capacity retained ratio (compared to the initial capacity) increased from 77% to 94% when the  $\gamma$ -BL concentration

was increased from 0 to 10 wt%. A higher  $\gamma$ -BL concentration promoted Li<sup>+</sup> mobility in the IL, facilitating the electrode redox reactions and thus leading to better cycle life.  $\gamma$ -BL can also enhance formation of a stable cathode/electrolyte interface film (as shown in Fig. 8), which suppresses detrimental irreversible side reactions, preventing capacity loss [47]. A similar result was found for the VC additive (to improve cell cyclability), as shown in Fig. S4 (in Supplementary Data). Clearly, at this relatively low temperature, the introduction of the additives to the IL electrolyte is beneficial for improving cell performance. However, an excessive addition should be avoided since it may cause a safety risk (as shown in Fig. 3(d)). Of note, the cell with the conventional organic electrolyte still exhibited superior cell durability (almost no decay after the same number of cycles). The IL needs to be further modified (i.e., redesign of the constituent cations and anions) to improve its room-

**Table 2**

Effects of additive type and concentration in 1 M LiTFSI/BMP–TFSI IL electrolyte on charge–discharge performance of Li/LiFePO<sub>4</sub> cells at 25 °C and 50 °C.

Concentration (wt%) in 1 M LiTFSI/ BMP–TFSI	Electrochemical performance							
	25 °C				50 °C			
	$\gamma$ -BL		VC		$\gamma$ -BL		VC	
Capacity at 0.1 C (mAh g <sup>-1</sup> )	Capacity retained ratio at 1 C (%)	Capacity at 0.1 C (mAh g <sup>-1</sup> )	Capacity retained ratio at 1 C (%)	Capacity at 0.1 C (mAh g <sup>-1</sup> )	Capacity retained ratio at 5 C (%)	Capacity at 0.1 C (mAh g <sup>-1</sup> )	Capacity retained ratio at 5 C (%)	
0	91	12	91	12	140	45	140	45
2.5	124	32	117	20	150	48	142	46
5	133	35	128	21	152	50	151	47
7.5	140	38	133	30	156	52	154	49
10	142	42	137	35	159	56	157	51

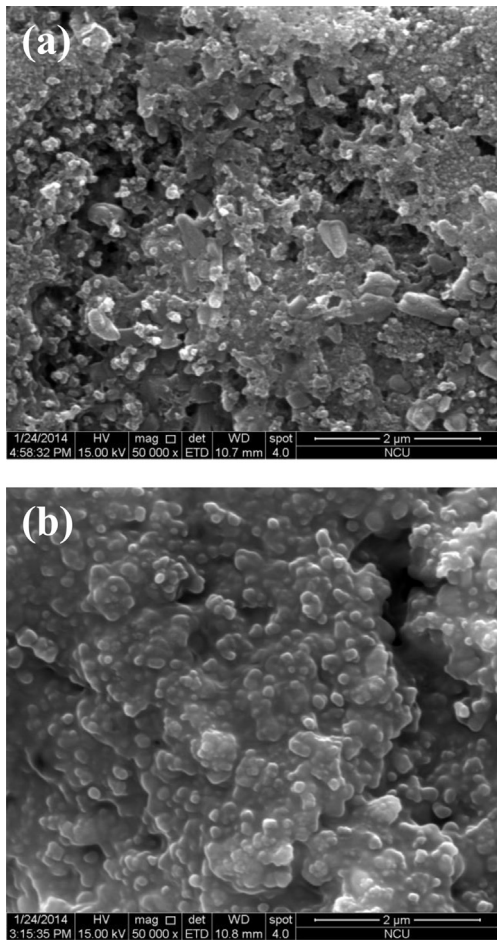


**Fig. 8.** SEM micrograph of the LiFePO<sub>4</sub> electrodes after cycling in IL electrolytes (a) without and (b) with 10 wt%  $\gamma$ -BL for 50 cycles at 25 °C.

temperature properties, especially when the cell high-rate and stability performance is of interest.

At 50 °C, as shown in Fig. 9(a) and (b), the maximum capacity (at 0.1 C) and the high-rate performance of the cells with IL-based electrolytes considerably improved (as compared to those at 25 °C in Fig. 7). Although increasing the  $\gamma$ -BL concentration (up to 10 wt %) increases both the properties, the benefits of the additive to performance enhancement are less significant than those found at 25 °C. This is associated with a great enhancement of Li<sup>+</sup> mobility in IL at the elevated temperature [31]; therefore, the role of the additive becomes less important. Effects of temperature on viscosity, conductivity, and  $T_{\text{Li}}^+$  of the electrolytes are shown in Figs. 5 and 6, and Table 1, respectively; the results indicate that the higher the temperature, the less influential of the additives. The Li/LiFePO<sub>4</sub> cell incorporating the IL electrolyte with 10 wt%  $\gamma$ -BL shows a maximum capacity of 159 mAh g<sup>-1</sup>; 56% of the capacity can be retained at a high rate of 5 C. Both these values are comparable to those (154 mAh g<sup>-1</sup> and 62%) obtained with the conventional organic electrolyte. Fig. 9(c) shows the cyclic stability of the Li/LiFePO<sub>4</sub> cells with various electrolytes evaluated at 50 °C. Interestingly, the cell with plain IL electrolyte shows the best durability. Great cyclability of LiFePO<sub>4</sub> cells with IL electrolytes was also reported [48,49]. The  $\gamma$ -BL additive, which may be unstable at such a temperature, had a negative effect on cell cyclability. When the additive concentration was increased from 0 to 10 wt%, the capacity loss after 100 cycles increased from almost zero to 15%. As shown, with the organic electrolyte, an ~18% capacity decay was

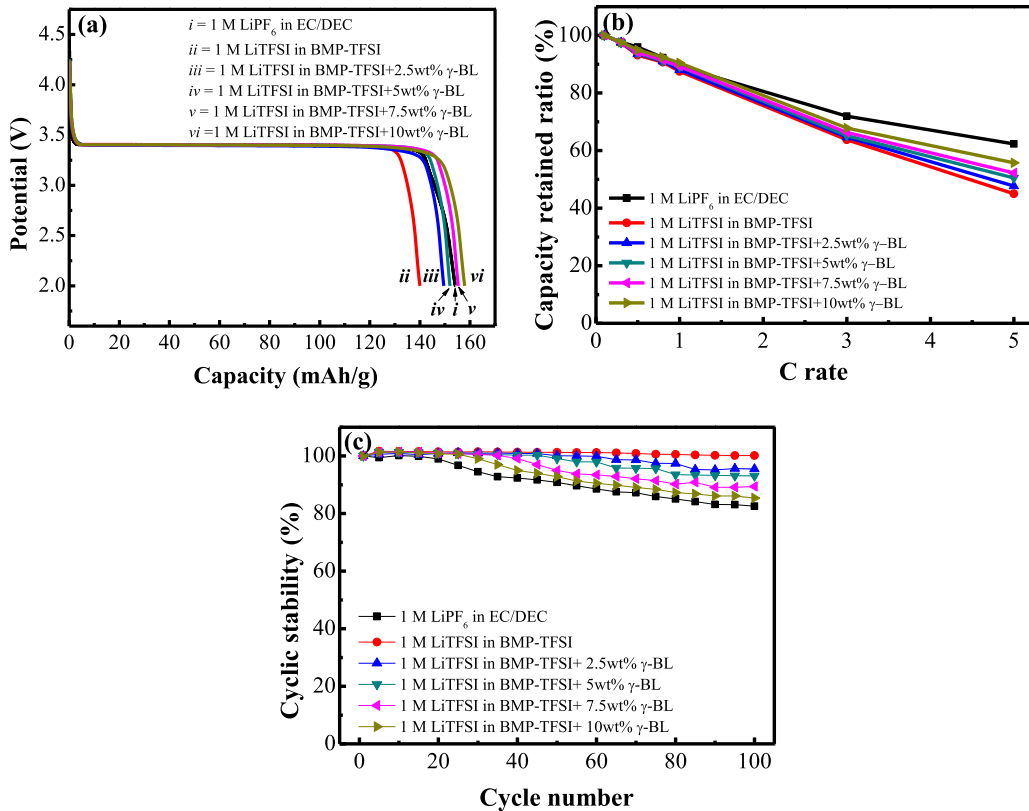
found after the same number of cycles. This is mainly due to undesirable interactions of the electrode/electrolyte, decomposition of LiPF<sub>6</sub>, and evaporation of the electrolyte at the elevated temperature [43,44,50]. The capacity, high-rate performance, and cyclic stability of the cells incorporating the VC-added IL electrolytes (with various VC concentrations) at 50 °C are shown in Fig. S5 (Supplementary Data); similar trends to those found for  $\gamma$ -BL were observed.

Fig. 10 summarizes the effects of temperature (25 °C, 50 °C, and 75 °C) on the cell performance for three kinds of electrolyte, namely the conventional organic electrolyte and IL electrolytes with and without 5 wt%  $\gamma$ -BL additive. As shown in Fig. 10(a), while the maximum capacities in the organic electrolyte and in the  $\gamma$ -BL-incorporated IL electrolyte decrease above 50 °C, the capacity in the plain IL continuously increases with temperature and becomes the highest among the cells at 75 °C. On the other hand, the high-rate performance of the organic-electrolyte and IL-based-electrolyte cells decreases and increases, respectively, with increasing temperature, as demonstrated in Fig. 10(b). At 75 °C, the capacity retained ratios at 3 C are 17%, 69%, and 77%, respectively, for the three electrolytes. At such a high temperature, the organic electrolyte and additive are volatile and unstable (according to the TGA data), and the IL (with a decomposition temperature of as high as ~400 °C) becomes less viscous and thus is favorable for ionic transport. As a result, use of the plain IL electrolyte (no additives) is recommended.

The capacity retained ratio after 100 charge–discharge cycles of the cells with the three electrolytes as a function of temperature is shown in Fig. 10(c). The capacity fading rate in the organic electrolyte clearly accelerates with increasing temperature, from ~0% to 36% when the temperature increases from 25 °C to 75 °C. In contrast, the cell with plain IL electrolyte shows improved cyclability at high temperature (almost no capacity decay was found at 75 °C after cycling). Raising the temperature increases the Li<sup>+</sup> transference number in the IL electrolyte (as Table 1), minimizing the unfavorable intercalation/deintercalation of BMP<sup>+</sup> and TFSI<sup>-</sup> into/from LiFePO<sub>4</sub>, which lead to electrode deterioration. The non-volatility and chemical benignity of ILs also contribute to the great electrode durability at high temperature. The cyclic performance of the cell with  $\gamma$ -BL-incorporated IL electrolyte is between the two extremes, regardless of the operation temperature. According to the data in Fig. 10, cell performance, such as maximum capacity, high-rate capability, and cyclic life, can be optimized via appropriate selection of the electrolyte composition for various-temperature applications.

#### 4. Conclusion

The LiTFSI/BMP–TFSI IL electrolyte shows high thermal stability and non-flammability and thus is promising for battery applications. Its high viscosity, low conductivity, and low  $T_{\text{Li}}^+$  (not desirable for Li/LiFePO<sub>4</sub> cells) at room temperature can be alleviated by the introduction of organic additives.  $\gamma$ -BL was found to be more effective than VC and PC in the IL electrolyte to improve cell capacity, rate capability, and cyclability. However, it should be noted that an excessive amount of additives (>10 wt%) increases electrolyte flammability. With increasing temperature, since the viscosity is reduced and the  $T_{\text{Li}}^+$  is increased, the advantages of the IL electrolyte become noticeable. Above 50 °C, the additives may not be necessary, because their instability would lead to adverse effects on cell performance (although their evaporation can be suppressed via better cell sealing). At 75 °C, the LiFePO<sub>4</sub> electrode shows a capacity of 152 mAh g<sup>-1</sup> (at 0.1 C) and a 72% capacity retention at 3 C in the plain IL electrolyte; furthermore, no noticeable performance fading was found after 100 charge–discharge cycles. These



**Fig. 9.** (a) Discharge curves at 0.1 C, (b) capacity retained ratios at various charge-discharge rates compared to that obtained at 0.1 C, and (c) cyclic stability of Li/LiFePO<sub>4</sub> cells incorporating a conventional organic electrolyte and IL electrolytes without and with various concentrations of  $\gamma$ -BL at 50 °C.

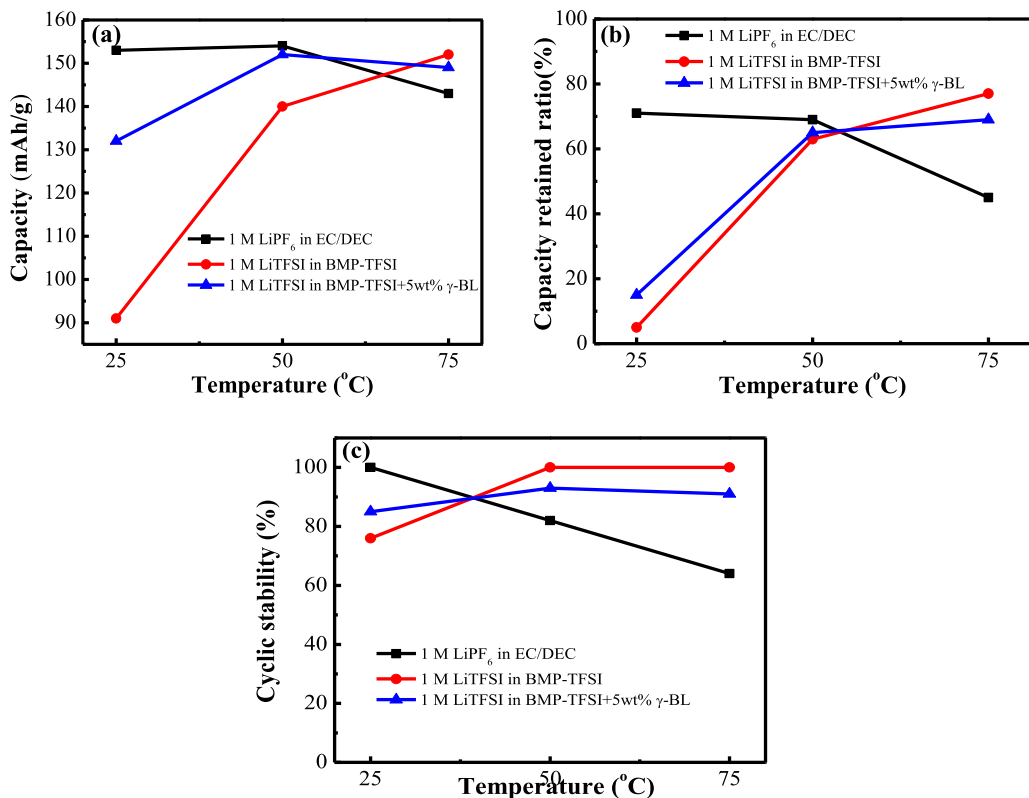


**Fig. 10.** Effects of temperature on (a) capacity at 0.1 C, (b) capacity retained ratios at 3 C compared to that obtained at 0.1 C, and (c) cyclic stability of Li/LiFePO<sub>4</sub> cells incorporating a conventional organic electrolyte and IL electrolytes without and with 5 wt%  $\gamma$ -BL.

properties are distinctly superior to those found for the conventional organic electrolyte. The IL electrolytes have shown great potential for high-safety applications especially at elevated temperatures.

## Acknowledgments

The financial support of this work by the National Science Council of Taiwan is gratefully appreciated.

## Appendix A. Supplementary data

Supplementary data related to this article can be found at <http://dx.doi.org/10.1016/j.jpowsour.2014.02.085>.

## References

- [1] W. van Schalkwijk, B. Scrosati (Eds.), *Advances in Lithium-ion Batteries*, Kluwer Academic/Plenum, Boston, 2004.
- [2] T. Tanaka, K. Ohta, N. Arai, *J. Power Sources* 97–98 (2001) 2–6.
- [3] T. Takamura, *Solid State Ionics* 152–153 (2002) 19–34.
- [4] K. Zaghib, P. Charest, A. Guerfi, J. Shim, M. Perrier, K. Striebel, *J. Power Sources* 134 (2004) 124–129.
- [5] R.A. March, S. Vukson, S. Sarampudi, B.V. Ratnakumar, M.C. Smart, M. Manzo, P.J. Dalton, *J. Power Sources* 97–98 (2001) 25–27.
- [6] P.G. Bruce, *Solid State Ionics* 179 (2008) 752–760.
- [7] Y. Nishi, *J. Power Sources* 100 (2001) 101–106.
- [8] J.B. Goodenough, K. Youngsik, *Chem. Mater.* 22 (2010) 587–603.
- [9] S.E. Sloop, J.K. Pugh, S. Wang, J.B. Kerr, K. Kinoshita, *Electrochem. Solid State Lett.* 4 (2001) A42–A44.
- [10] C. Arbizzani, G. Gabrielli, M. Mastragostino, *J. Power Sources* 196 (2011) 4801–4805.
- [11] B. Garcia, S. Lavallée, G. Perron, C. Michot, M. Armandbattery, *Electrochim. Acta* 49 (2004) 4583–4588.
- [12] M. Galiński, A. Lewandowski, I. Stepienak, *Electrochim. Acta* 51 (2006) 5567–5580.
- [13] D.M. Fox, W.H. Awad, J.W. Gilman, P.H. Maupin, H.C.D. Long, P.C. Trulove, *Green. Chem.* 5 (2003) 724–727.
- [14] A. Lewandowski, A.S. Mocek, *J. Power Sources* 194 (2009) 601–609.
- [15] J.S. Lee, J.Y. Bae, H. Lee, N.D. Quan, H.S. Kim, H. Kim, *J. Ind. Eng. Chem.* 10 (2004) 1086–1089.
- [16] N. Byrne, P.C. Howlett, D.R. MacFarlane, M.E. Smith, A. Howes, A.F. Hollenkamp, T. Bastow, P. Hale, M. Forsyth, *J. Power Sources* 184 (2008) 288–296.
- [17] N. Byrne, P.C. Howlett, D.R. MacFarlane, M. Forsyth, *Adv. Mater.* 17 (2005) 2497–2501.
- [18] C. Tiyapiboonchaiya, J.M. Pringle, J. Sun, N. Byrne, P.C. Howlett, D.R. MacFarlane, M. Forsyth, *Nat. Mater.* 3 (2004) 29–32.
- [19] J.H. Shin, E.J. Cairns, *J. Power Sources* 177 (2008) 537–545.
- [20] J.H. Shin, P. Basak, J.B. Kerr, E.J. Cairns, *Electrochim. Acta* 54 (2008) 410–414.
- [21] R.S. Kühnel, N. Böckenfeld, S. Passerini, M. Winter, A. Balducci, *Electrochim. Acta* 56 (2011) 4092–4099.
- [22] V. Chakrapani, F. Rusli, M.A. Filler, P.A. Kohl, *J. Phys. Chem. C* 115 (2011) 22048–22053.
- [23] L.E. Ouattara, R. Dedryvère, C. Siret, P. Biensan, D. Gonbeau, *J. Electrochem. Soc.* 156 (2009) A468–A477.
- [24] H. Sano, H. Sakaabe, H. Matsumoto, *J. Electrochem. Soc.* 158 (2011) A316–A321.
- [25] M. Li, B. Yang, Z. Zhang, L. Wang, Y. Zhang, *J. Appl. Electrochem.* 43 (2013) 515–521.
- [26] A. Chagnes, M. Diaw, B. Carre, P. Willmann, D. Lemordant, *J. Power Sources* 145 (2005) 82–88.
- [27] M. Diaw, A. Chagnes, B. Carré, P. Willmann, D. Lemordant, *J. Power Sources* 146 (2005) 682–684.
- [28] H.F. Xiang, B. Yin, H. Wang, H.W. Lin, X.W. Ge, S. Xie, C.H. Chen, *Electrochim. Acta* 55 (2010) 5204–5209.
- [29] H. Wang, S. Liu, N. Wang, Y. Liu, *Int. J. Electrochem. Sci.* 7 (2012) 7579–7586.
- [30] J. Reiter, J. Vondrák, J. Michálek, Z. Mička, *Electrochim. Acta* 52 (2006) 1398–1408.
- [31] F. Castiglione, E. Ragg, A. Mele, G.B. Appetecchi, M. Montanino, S. Passerini, *J. Phys. Chem. Lett.* 2 (2011) 153–157.
- [32] G.B. Appetecchi, M. Montanino, D. Zane, M. Carewska, F. Alessandrini, S. Passerini, *Electrochim. Acta* 54 (2009) 1325–1332.
- [33] N. Wongittharom, T.C. Lee, C.H. Hsu, G.T.K. Fey, K.P. Huang, J.K. Chang, *J. Power Sources* 240 (2013) 676–682.
- [34] G.T.K. Fey, K.P. Huang, H.M. Kao, *J. Power Sources* 196 (2011) 2810–2818.
- [35] F.F.C. Bazito, Y. Kawano, R.M. Torresi, *Electrochim. Acta* 52 (2007) 6427–6437.
- [36] J. Evans, C.A. Vincent, P.G. Bruce, *Polymer* 28 (1987) 2324–2328.
- [37] P.G. Bruce, J. Evans, C.A. Vincent, *Solid State Ionics* 28–30 (1988) 918–922.
- [38] D. Choi, P.N. Kumta, *J. Power Sources* 163 (2007) 1064–1069.
- [39] G.T.K. Fey, H.J. Tu, K.P. Huang, Y.C. Lin, H.M. Kao, S.H. Chan, *J. Solid State Electrochem.* 16 (2012) 1857–1862.
- [40] G.T.K. Fey, Y.G. Chen, H.M. Kao, *J. Power Sources* 189 (2009) 169–178.
- [41] C.Z. Lu, G.T.K. Fey, H.M. Kao, *J. Power Sources* 189 (2009) 155–162.
- [42] H.C. Shin, W. I Cho, H. Jang, *Electrochim. Acta* 52 (2006) 1472–1476.
- [43] T. Kawamura, S. Okada, J.I. Yamaki, *J. Power Sources* 156 (2006) 547–554.
- [44] X. Kang, *Chem. Rev.* 104 (2004) 4303–4417.
- [45] W.F. Howard, R.M. Spotnitz, *J. Power Sources* 165 (2007) 887–891.
- [46] K. Hayamizu, Y. Aihara, S. Arai, C.G. Martinez, *J. Phys. Chem. B* 103 (1999) 519–524.
- [47] X.Y. Zhang, S.H. Fang, Z.X. Zhang, L. Yang, *Chin. Sci. Bull.* 56 (2011) 2906–2910.
- [48] A.P. Lewandowski, A.F. Hollenkamp, S.W. Donne, A.S. Best, *J. Power Sources* 195 (2010) 2029–2035.
- [49] G.T. Kima, S.S. Jeong, M.Z. Xue, A. Balducci, M. Winter, S. Passerini, F. Alessandrini, G.B. Appetecchi, *J. Power Sources* 199 (2012) 239–246.
- [50] M. Koltypin, D. Aurbach, L. Nazar, B. Ellis, *Electrochim. Solid State Lett.* 10 (2007) A40–A44.